

***Research Quarterly
for Exercise and Sport***

**Validity of neural networks to determine body position on
the bicycle**

| | |
|----------------------|---|
| Journal: | <i>Research Quarterly for Exercise and Sport</i> |
| Manuscript ID | 21-05-BIMB-06.R2 |
| Manuscript Type: | Original Article |
| Manuscript Category: | Biomechanics and Motor Behavior |
| Keyword: | Biomechanics, Technology, Quantitative study, Kinesiology |
| | |

SCHOLARONE™
Manuscripts

Validity of neural networks to determine body position on the bicycle

Authors

Rodrigo Rico Bini¹, Gil Serrancoli², Paulo Roberto Pereira Santiago³, Allan Pinto⁴, Felipe Moura⁵

¹Rural Health School, La Trobe University, Australia

²Department of Mechanical Engineering, Universitat Politècnica de Catalunya, Spain

³School of Physical Education and Sport of Ribeirão Preto, University of São Paulo, Brazil

⁴Institute of Computing, State University of Campinas, Brazil

⁵State University of Londrina, Brazil

Name and address for correspondence

Dr. Rodrigo Bini

Rural Health School

La Trobe University

Flora Hill Campus

Postal code: 3550

Phone (64) 03 5444 7466

Email: r.bini@latrobe.edu.au

Funding: Grant #2019/17729-0, São Paulo Research Foundation (FAPESP)

IRB Approval: HEC19001

Acknowledgements: Authors acknowledge all cyclists who took part in this study and, grant #2019/17729-0, São Paulo Research Foundation (FAPESP).

Keywords: Biomechanics, Technology, Quantitative study, Kinesiology

Words count: Abstract (199 words) and body of the text (3468 words without abstract and references).

Figures: 3

Tables: 1

Abstract

With the increased access to neural networks trained to estimate body segments from images and videos, this study assessed the validity of some of these networks in enabling the assessment of body position on the bicycle. Fourteen cyclists pedalled stationarily in one session on their own bicycles whilst video was recorded from their sagittal plane. Reflective markers attached to key bony landmarks were used to manually digitise joint angles at two positions of the crank (3 o'clock and 6 o'clock) extracted from the videos (Reference method). These angles were compared to measurements taken from videos generated by two deep learning-based approaches designed to automatically estimate human joints (Microsoft Research Asia-MSRA and OpenPose). Mean bias for OpenPose ranged between 0.03-1.81° whilst the MSRA method presented errors between 2.29-12.15°. Correlation coefficients were stronger for OpenPose than for the MSRA method in relation to the Reference method for the torso ($r = 0.94$ vs. 0.92), hip ($r = 0.69$ vs. 0.60), knee ($r = 0.80$ vs. 0.71) and ankle ($r = 0.23$ vs. 0.20). OpenPose presented better accuracy than the MSRA method in

43 determining body position on the bicycle but both methods seem comparable to assess implications
44 from changes in bicycle configuration.

45 **Keywords:** Biomechanics, Technology, Quantitative study, Kinesiology

46

47 Introduction

48 Bicycle fitting is a method utilised to optimise the position of the bicycle to the cyclist (Bini et al., 2014),
49 which involves a range of measurements to assess cyclists' posture on their bicycles. Amongst the
50 most recommended techniques to assess body position on the bicycle, analysis of joint angles from
51 video recording has been largely used as it allows for bicycle fitting to be further individualised (Fonda
52 et al., 2014; Swart & Holliday, 2019). However, accurate measurements of angles involve determining
53 joint centres from manual palpation and markup of bony landmarks on the skin (Malus et al., 2021),
54 which can be prone to errors depending on the experience of the assessor (Sinclair et al., 2014).
55 Nevertheless, whenever markers are properly attached to bony landmarks they are considered a gold
56 standard method.

57 The use of marker-less methods to extract joint centres from video has been attempted in several
58 studies (Grigg et al., 2018; Needham et al., 2017; Ong et al., 2017; Serrancolí et al., 2020). Ong et al.
59 (2017) observed differences of $<1^\circ$ for various joint angles using a marker-less tracking system during
60 walking and jogging, demonstrating promising outcomes. More recently, the use of convolution neural
61 networks (CNN) trained on large image datasets (Cao et al., 2021) improved human pose estimation
62 and joint centre identification. These methods involve the use of images from people performing
63 various movements (i.e. walking, jumping, dancing, etc.) that are labelled to determine body segments
64 and joints (i.e. keypoints) and used for training a computer program to automatically identify similar
65 patterns in new images. However, only Serrancoli et al. (2020) utilised CNN-based approaches to
66 identify segmental movement and joint centres during cycling. This application is important as it can
67 further allow for marker-less methods to determine cyclists' position on the bicycle and potentially
68 inform bicycle fitting. However, comparison with criterion methods (i.e. marker-based) is lacking given
69 neural networks use different assumptions in determining joint centres (i.e. methods to determine
70 body segments). This provides an opportunity to utilise pre-trained networks that can determine
71 human body segments and joints to the analysis of cycling.

72 Body position on the bicycle has largely involved determining upper and lower limb angles at key parts
73 of the crank cycle. As an example, the 6 o'clock (Bini, 2020; Peveler & Green, 2011; Priego Quesada et
74 al., 2016) and the 3 o'clock positions of the crank cycle (Bini & Hume, 2016; Bini, Hume, & Croft, 2014)
75 were utilised. The main rationale for choosing these positions is because, the 6 o'clock is close to the
76 maximum extension of the lower limbs (Holmes et al., 1994) and the 3 o'clock is close to peak pedal
77 power (Martin & Brown, 2009). Therefore, examining joint angles at these positions can help
78 differentiate cycling posture (Bini, P.A. Hume, & Croft, 2014). However, the use of marker-less motion
79 analysis methods has not been assessed in terms of their accuracy in determining cyclists' posture.
80 The use of marker-less as part of bicycle fitting assessment using video-calls can be helpful because
81 the restrictions from COVID-19 have limited face-to-face non-essential activities globally. Moreover,
82 utilising freely available pre-trained networks could accelerate the use of these automated methods
83 by practitioners, reducing barriers such as image labelling, network retraining, etc.

84 Therefore, the aim of this study was to compare a marker-based method for estimating joint angles
85 on the bicycle (i.e. Reference) with two open-source convolutional neural networks (Cao et al., 2021;
86 Xiao et al., 2018) designed to perform the same task automatically. Given these pre-trained networks

87 are normally trained using images from people performing a wide range of movements (e.g. walking,
88 jumping, dancing, etc.), our hypothesis was that both methods should provide practically acceptable
89 measurements of body position on the bicycle (i.e. joint angles). Therefore, broad learning obtained
90 from both networks should be appropriate to detect body segments in cycling-related images.

91

92 **Materials and methods**

93 Fourteen male cyclists (33 ± 7 years of age, 176 ± 6 cm of stature and 74 ± 8 kg of body mass) ranging
94 from recreational to competitive were assessed in a single session using their own bicycles (road,
95 triathlon, or mountain bike). They were engaged in road, triathlon or mountain bike training covering
96 5 ± 3 hours and 128 ± 65 km of cycling training per week at the time of the study. We based our sample
97 size calculation at the intention to determine a minimum difference of 5° in angles, which is at the
98 centre of the range proposed to determine body position on the bicycle (i.e. 10° , Millour et al., 2019;
99 Swart & Holliday, 2019). We also assumed that the within-cyclist's variability in angles would be 3.4°
100 (Bini & Hume, 2016), resulting in an effect size of 1.47. Our sample size calculation involved a
101 comparison of paired samples when $\alpha = 0.05$ and the power of the test is 0.80 using G*Power
102 statistical package (Faul et al., 2007). Before data collection, all cyclists signed an informed consent to
103 participate in the study, which was approved by the University Human Ethics Committee (XXXXX).

104 After measurements of stature and body mass, cyclists performed 2-min of cycling on their own
105 bicycles attached to a home cycle trainer (Active Intent Fitness Bike Trainer, NZ) at self-selected
106 cadence. A high-speed camera (Exilim EX-FC150, Casio Computer CO, Tokyo, Japan) was positioned at
107 the height of their saddle, 4-m away from the bicycles to record movement in the sagittal plane.
108 Reflective markers were positioned at the acromion, greater trochanter, lateral femoral epicondyle,
109 lateral malleolus and the head of the fifth metatarsal bone (Figure 1). Videos were recorded for 20-s
110 at the end of the 2-min of exercise at 120 fps (640x480 of frame resolution) using automated quick
111 shutter and anti-shake settings to minimise blur.

112 In this study, we compared the OpenPose (bottom-up) and the Microsoft Research Asia (MSRA - top-
113 down) methods, deep learning-based approach designed to estimate human pose and joint angles, in
114 the context of bicycle fitting. The bottom-up method relies on existing data to train the network whilst
115 the top-down method uses current learning to improve the accuracy of the network in future
116 predictions. The MSRA method first detects the location of people in an image, and then the body
117 segments for each detected person. Individuals and their respective body segments are detected using
118 the Mask RCNN framework (He et al., 2020), which is a two-stage approach where in the first stage,
119 images are scanned to determine areas likely to contain an object whilst the second stage classifies
120 these areas and generates bounding boxes and masks (i.e. removing surroundings). To associate each
121 person, and its body segments with detections from consecutive frames, the authors proposed a
122 tracking algorithm that takes advantage of temporal information via optical flow technique (Teed &
123 Deng, 2020). This involves extrapolating future position of segments during sequential movement
124 from historical data (i.e. bottom-up approach). OpenPose introduced the concept of association
125 scores via Part Affinity Fields (PAFs), which is a set of vector fields that determines the location and
126 orientation of body segments. The vector fields allow the estimation of a degree of association
127 between body segments. OpenPose computes a confidence map that informs the location of the body
128 segments and a set of vector fields (PAFs). Finally, both the confidence map and PAFs are fused by a
129 greedy inference strategy to estimate the final set of joints (i.e. optimisation of joint locations), for
130 each person in the image.

131 Video files were then imported to a customised program adapted from a freely available [code](#). This
132 code implements the Microsoft Research Asia (MSRA) method (Xiao et al., 2018) in MATLAB (R2021a,
133 MathWorks Inc, Natick, MA, USA). In this study, we used a model pre-trained in the COCO Consortium
134 ([cocodataset.org](#)) (Lin et al., 2014), which involves annotation of 250,000 people with segments
135 identified in a broad range of movements such as walking, jumping and dancing, as examples. Video
136 files were generated where the joint centres (i.e. keypoints) and body segments were identified by
137 the pre-trained neural network. The same process was conducted using the OpenPose method (Cao
138 et al., 2021), which is also pre-trained in the COCO dataset. Videos generated by the MSRA and the
139 OpenPose methods were later utilised to manually digitise torso, hip, knee and ankle angles in two
140 parts of the crank cycle (3 o'clock and 6 o'clock), as shown in Figure 1. As a reference method, videos
141 with the reflective markers only were utilised. Raw videos (i.e. Reference method) and pre-trained
142 neural network generated videos were imported to ImageJ (National Institute of Health, USA) where
143 a single experienced assessor measured the angles across five consecutive cycles. Even though both
144 pre-trained neural networks estimated joint coordinates, we followed a method utilised in clinics and
145 bike fitting, where angles are manually measured from pre-located joint positions on the video (e.g.
146 [Bike Fast Fit - Video Bike Fitting](#)). This process enables the identification of angles in key areas of the
147 crank cycle without a requirement of tracking multiple video frames. Because the MSRA did not track
148 the foot, the ankle angle was measured using the head of the fifth metatarsal bone marker for all
149 methods.

150 *****Figure 1*****

151 Differences in mean angles from each cyclist between manually placed markers and joint position
152 predicted by the neural network methods in relation to the Reference method were determined using
153 paired samples t-tests for each crank position. Magnitude of differences were assessed using Cohen's
154 effect sizes (d). Whenever $p < 0.05$ and $d > 0.80$, practically important differences were assumed from
155 the data. Mean bias and confidence interval for the differences (CI95) were calculated as part of the
156 Bland-Altman method (Bland & Altman, 1986) and Pearson correlations were computed to assess
157 association between methods. R values were ranked as poor (0–0.5), moderate (0.5–0.75), good
158 (0.75–0.90), and excellent (> 0.9) (Dancey & Reidy, 2004). Statistical analyses were conducted using
159 customised spreadsheets (Excel, Microsoft Inc, USA) and GraphPad Prism (Version 9.0.2, GraphPad
160 Software, San Diego, California USA).

161

162 **Results**

163 Significant differences were observed between angles from the MSRA method in comparison to the
164 Reference method, at the 3 o'clock crank position, for the torso ($p < 0.01$, $d = 0.38$), hip ($p < 0.01$, $d =$
165 1.93), knee ($p < 0.01$, $d = 1.52$) and ankle ($p = 0.01$, $d = 1.05$). No differences though were observed
166 between angles from the OpenPose and the Reference method (torso $p = 0.09$, hip $p = 0.12$, knee $p =$
167 0.69 , ankle $p = 0.36$). Angular data are presented in Table 1.

168 ****Table 1*****

169 Mean bias [CI95] between angles from the MSRA method compared to the Reference method at the
170 3 o'clock position was -2.6° [-8.0;2.8] for the torso, 8.9° [0.8; 16.9] for the hip, 12.1° [-0.3; 24.6] for
171 the knee and 7.8° [-11.3; 26.9] for the ankle. Mean bias [CI95] between angles from the OpenPose
172 method in comparison to the Reference method at the 3 o'clock position was 1.5° [-4.6;7.6] for the
173 torso, 1.4° [-4.9; 7.8] for the hip, 0.4° [-7.7; 8.6] for the knee and -1.5° [-13.3; 10.2] for the ankle.
174 Correlation coefficients were stronger for the OpenPose method than for the MSRA method in relation

175 to the Reference method for the torso ($r = 0.94$ vs. 0.92 - excellent), hip ($r = 0.69$ vs. 0.60 - moderate),
176 knee ($r = 0.80$ - good vs. 0.71 - moderate) and ankle ($r = 0.23$ vs. 0.20 - poor). Bland-Altman's plots
177 illustrate these outcomes in Figure 2.

178 *****Figure 2*****

179 Significant differences were observed between angles from the MSRA method in comparison to the
180 Reference method, at the 6 o'clock crank position, for the torso ($p < 0.01$, $d = 0.67$), hip ($p = 0.01$, $d =$
181 0.52) and knee ($p = 0.02$, $d = 0.46$). No differences were observed for the ankle ($p = 0.10$). No
182 differences were observed between angles from the OpenPose method and the Reference method
183 (torso $p = 0.08$, hip $p = 0.97$, knee $p = 0.09$, ankle $p = 0.28$). Angular data are presented in Table 1.

184 Mean bias [CI95] between angles from the MSRA method in comparison to the Reference method at
185 the 6 o'clock position was -4.4° [-12.8 ; 3.9] for the torso, 2.3° [-2.9 ; 7.5] for the hip, 4.3° [-7.7 ; 16.3]
186 for the knee and 3.3° [-10.7 ; 17.4] for the ankle. Mean bias [CI95] between angles from the OpenPose
187 method in comparison to the Reference method at the 6 o'clock position was 1.81° [-5.1 ; 8.7] for the
188 torso, -0.1° [-4.3 ; 4.3] for the hip, 1.5° [-4.8 ; 8.0] for the knee and -1.2° [-9.1 ; 6.7] for the ankle.
189 Correlation coefficients were stronger for the OpenPose method than for the MSRA method in relation
190 to the Reference method for the torso ($r = 0.94$ - excellent vs. 0.79 - good), hip ($r = 0.86$ vs. 0.82 -
191 good), knee ($r = 0.91$ - excellent vs. 0.82 - good) and ankle ($r = 0.87$ vs. 0.75 - good). Bland-Altman's
192 plots illustrate these outcomes in Figure 3.

193 *****Figure 3*****

194

195 Discussion

196 The purpose of this study was to compare joint angles on the bicycle assessed using pre-trained neural
197 networks with outputs from a marker-based method. The hypothesis was that both methods would
198 provide practically acceptable measurements of joint angles due to similarities in body position. The
199 data demonstrated that the OpenPose method presented greater accuracy than the MSRA method in
200 determining body position on the bicycle. Mean bias for the OpenPose method ranged between 0.03 -
201 1.81° whilst the MSRA method presented errors between 2.29 - 12.15° . Ong et al. (2017) observed
202 differences of $< 1^\circ$ for various joint angles using a marker-less tracking system during walking and
203 jogging. During cycling, intra-session errors in joint angles have been shown to vary between < 1 - 3°
204 (Bini & Hume, 2020), which suggests that differences between the OpenPose method could be
205 negligible but the MSRA method presented larger errors. These findings are novel because they
206 demonstrate that an automated marker-less method (i.e. OpenPose) can accurately determine joint
207 angles and help assess body position on the bicycle.

208 The assessment of joint angles during bicycle fitting is based on the fact that changes in bicycle
209 configuration affect movement patterns (Bini, Hume, & Kilding, 2014; Menard et al., 2020). This means
210 that, accuracy in determining joint angles is important to ensure that the position of the cyclist on the
211 bicycle aligns with the intention of the fitting process. Differently though, changes in joint angles of
212 ~ 10 - 14° when saddle position is modified have not been associated with changes in internal forces
213 (Bini & Hume, 2014). This indicates that, errors in determining knee angles may not result in large
214 differences in bicycle configuration. It is also possible that errors in determining bicycle configuration
215 (e.g. using the MSRA method) may not result in differences in perceived comfort (Bini, 2020; Priego
216 Quesada et al., 2016). We can also speculate that these errors may only affect internal forces in parts
217 of the crank cycle where joint loads are low (Bini, 2021). Therefore, further studies are needed to

218 explore the implications of determining saddle position, for example, using automated marker-less
219 methods. This is particularly important in light of the poor correlation between both methods and the
220 Reference method for the ankle joint at the 3 o'clock position.

221 In this study, joint angles were measured in two key positions of the crank cycle, which limits the
222 conclusion on whether automated methods can accurately track motion. It is possible that, in some
223 parts of the crank cycle, errors in identifying body segments may be larger. As an example, the 3
224 o'clock position presented larger errors than the 6 o'clock position for the MSRA method, which can
225 be potentially associated with the right and left limbs having a very distinct position at the 6 o'clock
226 but a more similar position at the 3 o'clock, leading the automated method to swap sides of the
227 skeleton. This though was not the case for the OpenPose method as errors were not largely different
228 between crank positions. As neural networks are normally trained using a broad range of images or
229 people moving (i.e. walking, jumping, dancing, etc.), the straight leg observed at the 6 o'clock
230 potentially increases the accuracy of the networks to determine the skeleton. Therefore, training
231 neural networks with cycling related images is important to further enhance the accuracy of the
232 network, particularly when using data to determine joint loads.

233 It is important to note that both CNN-based methods were designed considering largely non-cycling-
234 related scenarios since they were based on COCO and MPII datasets. According to Cao et al. (Cao et
235 al., 2021), the MSRA method outperformed the OpenPose in 12.3 percentual points, considering the
236 test set of the COCO dataset. However, our study demonstrates that OpenPose outperformed MSRA
237 when using cycling-related images. The MRSA networks has been trained to analyse images with a
238 resolution of 256x192 pixels whilst the OpenPose network used the whole image resolution. This
239 means that, OpenPose had increased resolution at each frame to determine joint keypoints,
240 potentially explaining its increased accuracy. Our results suggest that the vector fields (PAFs), which
241 encode the location and orientation of body segments, were more effective in determining the
242 segments of a person in cycling-related images than the optical flow-based approach used in the MSRA
243 method. This means that, when using optical flow to determine sequential movement, the MSRA
244 presented lower capacity than the OpenPose method to determine the joints. We believe that these
245 results are valuable for computer scientists and engineers when designing AI-based methods for
246 detecting human pose and joints. The use of the OpenPose to inform bicycle fitting provides an
247 opportunity to streamline the analysis of posture on the bicycle and automate the extraction of
248 quantitative outcomes (i.e. joint angles).

249 The use of a two-dimensional model is a very popular method of obtaining angles from cyclists in
250 clinical and sports settings due to the easy access to video recording capability through smartphones.
251 However, it is known that two-dimensional data presented $\sim 2.2 \cdot 10^\circ$ of error in relation to three-
252 dimensional data (Fonda et al., 2014; Umberger & Martin, 2001). Therefore, it is important that, if
253 automated methods are used, errors in determining joint angles via two-dimensional analysis do not
254 increase further the known limitations of sagittal plane analyses. Further studies should explore if the
255 use of three-dimensional marker-less methods are feasible to analyse cycling motion, as they showed
256 promising results in other movements (D'Antonio et al., 2021; Kanko et al., 2021).

257 Angles presented in this study were manually digitised from the video footage, which may add errors
258 to the true measurement of joint angles. However, this element has been shown to increase to a trivial
259 magnitude (i.e. $< 1.5^\circ$) bias in measuring joint angles in cyclists (Bini & Hume, 2016) and should be
260 equivalent between methods as all involved manual digitisation of angles. Therefore, future studies
261 should compare intra-cycle data between methods to assess the extent of differences. It is also
262 important to note that cyclists pedalled at self-selected sub-maximal intensity and cadence, which

263 limits the assumption that the automated methods will perform similarly during higher intensity
264 cycling (e.g. sprinting). Clean background was used but it is unclear if the automated method would
265 cope with data obtained in outdoor settings. Moreover, the use of online technology to assess cyclists
266 remotely (e.g. Zoom, Gmeet, etc) can facilitate bicycle fitting to be conducted via distance but it is
267 unclear if elements such as background and position and orientation of the camera would affect the
268 accuracy of the automated methods. Videos from this study were collected with standard (640x480
269 pixels) frame resolution at high frame rate (120 fps), which is limited compared to some modern
270 cameras. Whilst some smartphones enable slow motion (i.e. high frame rate) to be recorded in high
271 resolution, webcams are limited to 60 fps, with unclear implications on the performance of the
272 automated methods. Therefore, future studies should explore changing camera settings in order to
273 assess if outcomes from the automated method remain appropriate.

274 The use of public available codes to automate human pose estimation was also implemented in this
275 study without changes to the original code. One improvement that should be attempted in future use
276 involves filtering and interpolating the joint coordinates as noise was visually observed in the videos
277 leading the automated methods to misinterpret the location of joint centres. These corrections have
278 been utilised in prior research (Serrancolí et al., 2020) and should improve the quality of the data,
279 particularly when temporal patterns are explored. In addition, exploring accuracy of these networks
280 when videos are recorded at lower frame rate and/or with less image resolution should benefit further
281 use of these methods.

282 The conclusion is that the OpenPose method presented improved accuracy compared to the MSRA
283 method in determining body position on the bicycle but both methods seem feasible to assess
284 implications from changes in bicycle configuration. The OpenPose method though should be
285 preferably used when higher accuracy in determining joint angles is required.

286

287

288 **Declaration of interest statement**

289 The authors declare no conflict of interest with the content of this paper.

290 **References**

- 291 Bini, R. (2021, 2021/02/01). Influence of saddle height in 3D knee loads commuter cyclists: A
292 statistical parametric mapping analysis. *Journal of Sports Sciences*, 39(3), 275-288.
293 <https://doi.org/10.1080/02640414.2020.1816289>
- 294
295 Bini, R., & Hume, P. (2020). Reproducibility of lower limb motion and forces during stationary
296 submaximal pedalling using wearable motion tracking sensors. *Sports Biomechanics*, 1-22.
297 <https://doi.org/10.1080/14763141.2020.1776760>
- 298
299 Bini, R. R. (2020, 2020/06/01). Acute effects from changes in saddle height in perceived comfort
300 during cycling. *International Journal of Sports Science & Coaching*, 15(3), 390-397.
301 <https://doi.org/10.1177/1747954120918965>
- 302
303 Bini, R. R., & Hume, P. (2016). A Comparison of Static and Dynamic Measures of Lower Limb Joint
304 Angles in Cycling: Application to Bicycle Fitting. *Human Movement*, 17(1), 36-42.
305 <https://doi.org/10.1515/humo-2016-0005>
- 306
307 Bini, R. R., & Hume, P. A. (2014). Effects of saddle height on knee forces of recreational cyclists with
308 and without knee pain. *International SportMed Journal*, 15(2), 188-199.
309 https://doi.org/https://www.researchgate.net/publication/263587378_EFFECTS_OF_SADDLE_HEIGHT_ON_KNEE_FORCES_OF_RECREATIONAL_CYCLISTS_WITH_AND_WITHOUT_KNEE_PAIN
- 310
311 PAIN
- 312
313 Bini, R. R., & Hume, P. A. (2016). A comparison of static and dynamic measures of lower limb joint
314 angles in cycling: Application to bicycle fitting. *Human Movement*, 17(1), 36-42.
315 <https://doi.org/10.1515/humo-2016-0005>
- 316
317 Bini, R. R., Hume, P. A., Croft, J., & Kilding, A. (2014). Optimizing Bicycle Configuration and Cyclists'
318 Body Position to Prevent Overuse Injury Using Biomechanical Approaches. In R. R. Bini & F.
319 P. Carpes (Eds.), *Biomechanics of Cycling* (pp. 71-83). Springer International Publishing.
320 https://doi.org/10.1007/978-3-319-05539-8_8
- 321
322 Bini, R. R., Hume, P. A., & Croft, J. L. (2014). Cyclists and triathletes have different body positions on
323 the bicycle. *European Journal of Sport Science*, 14(S1), S109-S115.
324 <https://doi.org/10.1080/17461391.2011.654269>
- 325
326 Bini, R. R., Hume, P. A., & Kilding, A. E. (2014). Saddle height effects on pedal forces, joint mechanical
327 work and kinematics of cyclists and triathletes. *European Journal of Sport Science*, 14(1), 44-
328 52. <https://doi.org/10.1080/17461391.2012.725105>
- 329
330 Cao, Z., Hidalgo, G., Simon, T., Wei, S. E., & Sheikh, Y. (2021). OpenPose: Realtime Multi-Person 2D
331 Pose Estimation Using Part Affinity Fields. *IEEE Transactions on Pattern Analysis and*
332 *Machine Intelligence*, 43(1), 172-186. <https://doi.org/10.1109/TPAMI.2019.2929257>
- 333

- 334 D'Antonio, E., Taborri, J., Mileti, I., Rossi, S., & Patané, F. (2021). Validation of a 3D Markerless
335 System for Gait Analysis Based on OpenPose and Two RGB Webcams. *IEEE Sensors Journal*,
336 21(15), 17064-17075. <https://doi.org/10.1109/JSEN.2021.3081188>
- 337
- 338 Dancy, C., & Reidy, J. (2004). *Statistics Without Maths for Psychology with Psychology Dictionary*.
339 Pearson Education, Limited. <https://books.google.com.au/books?id=LwQtPQAACAAJ>
- 340
- 341 Faul, F., Erdfelder, E., Lang, A.-G., & Buchner, A. (2007, 2007/05/01). G*Power 3: A flexible statistical
342 power analysis program for the social, behavioral, and biomedical sciences. *Behavior*
343 *Research Methods*, 39(2), 175-191. <https://doi.org/10.3758/BF03193146>
- 344
- 345 Fonda, B., Sarabon, N., & Li, F.-X. (2014, 2014/06/15). Validity and reliability of different kinematics
346 methods used for bike fitting. *Journal of Sports Sciences*, 32(10), 940-946.
347 <https://doi.org/10.1080/02640414.2013.868919>
- 348
- 349 Grigg, J., Haakonssen, E., Rathbone, E., Orr, R., & Keogh, J. W. L. (2018, 2018/07/03). The validity and
350 intra-tester reliability of markerless motion capture to analyse kinematics of the BMX
351 Supercross gate start. *Sports Biomechanics*, 17(3), 383-401.
352 <https://doi.org/10.1080/14763141.2017.1353129>
- 353
- 354 He, K., Gkioxari, G., Dollár, P., & Girshick, R. (2020). Mask R-CNN. *IEEE Transactions on Pattern*
355 *Analysis and Machine Intelligence*, 42(2), 386-397.
356 <https://doi.org/10.1109/TPAMI.2018.2844175>
- 357
- 358 Holmes, J. C., Pruitt, A. L., & Whalen, N. J. (1994). Lower extremity overuse in bicycling. *Clinics in*
359 *Sports Medicine*, 13(1), 187-203. <https://doi.org/www.sportsmed.theclinics.com/>
- 360
- 361 Kanko, R. M., Laende, E., Scott Selbie, W., & Deluzio, K. J. (2021, 2021/04/08/). Inter-session
362 repeatability of markerless motion capture gait kinematics. *Journal of Biomechanics*,
363 110422. <https://doi.org/https://doi.org/10.1016/j.jbiomech.2021.110422>
- 364
- 365 Lin, T.-Y., Maire, M., Belongie, S., Hays, J., Perona, P., Ramanan, D., Dollár, P., & Zitnick, C. L. (2014,
366 2014//). Microsoft COCO: Common Objects in Context. *Computer Vision – ECCV 2014*, Cham.
- 367
- 368 Malus, J., Skypala, J., Silvernail, J. F., Uchytíl, J., Hamill, J., Barot, T., & Jandacka, D. (2021). Marker
369 Placement Reliability and Objectivity for Biomechanical Cohort Study: Healthy Aging in
370 Industrial Environment (HAIE—Program 4). *Sensors*, 21(5).
371 <https://doi.org/10.3390/s21051830>
- 372
- 373 Martin Bland, J., & Altman, D. (1986). Statistical methods for assessing agreement between two
374 methods of clinical measurement. *The Lancet*, 327(8476), 307-310.
375 [https://doi.org/10.1016/S0140-6736\(86\)90837-8](https://doi.org/10.1016/S0140-6736(86)90837-8)
- 376

- 377 Martin, J. C., & Brown, N. A. T. (2009). Joint-specific power production and fatigue during maximal
378 cycling. *Journal of Biomechanics*, 42(4), 474-479.
379 <https://doi.org/10.1016/j.jbiomech.2008.11.015>
- 380
- 381 Menard, M., Domalain, M., Decatoire, A., & Lacouture, P. (2020, 2020/03/03). Influence of saddle
382 setback on knee joint forces in cycling. *Sports Biomechanics*, 19(2), 245-257.
383 <https://doi.org/10.1080/14763141.2018.1466906>
- 384
- 385 Millour, G., Duc, S., Puel, F., & Bertucci, W. (2019). Comparison of static and dynamic methods based
386 on knee kinematics to determine optimal saddle height in cycling. *Acta Bioeng Biomech*,
387 21(4), 93-99.
- 388
- 389 Needham, L., Long, M. J., & Irwin, G. (2017). *MARKERLESS MOTION CAPTURE WITHIN SPORT: AN*
390 *EXPLORATORY CASE STUDY* ISBS,
- 391
- 392 Ong, A., Harris, I. S., & Hamill, J. (2017, 2017/07/27). The efficacy of a video-based marker-less
393 tracking system for gait analysis. *Computer Methods in Biomechanics and Biomedical*
394 *Engineering*, 20(10), 1089-1095. <https://doi.org/10.1080/10255842.2017.1334768>
- 395
- 396 Peveler, W. W., & Green, J. M. (2011). Effects of saddle height on economy and anaerobic power in
397 well-trained cyclists. *Journal of Strength and Conditioning Research*, 25(3), 629-633.
398 <https://doi.org/10.1519/JSC.0b013e3181d09e60>
- 399
- 400 Priego Quesada, J. I., Pérez-Soriano, P., Lucas-Cuevas, A. G., Salvador Palmer, R., & Cibrián Ortiz de
401 Anda, R. M. (2016). Effect of bike-fit in the perception of comfort, fatigue and pain. *Journal*
402 *of Sports Sciences*, 35(14), 1459-1465. <https://doi.org/10.1080/02640414.2016.1215496>
- 403
- 404 Serrancolí, G., Bogatkov, P., Huix, J. P., Barberà, A. F., Egea, A. J. S., Ribé, J. T., Kanaan-Izquierdo, S.,
405 & Susín, A. (2020). Marker-Less Monitoring Protocol to Analyze Biomechanical Joint Metrics
406 During Pedaling. *IEEE Access*, 8, 122782-122790.
407 <https://doi.org/10.1109/ACCESS.2020.3006423>
- 408
- 409 Sinclair, J., Hebron, J., & Taylor, P. J. (2014, 2014/09/01/). The influence of tester experience on the
410 reliability of 3D kinematic information during running. *Gait & Posture*, 40(4), 707-711.
411 <https://doi.org/https://doi.org/10.1016/j.gaitpost.2014.06.004>
- 412
- 413 Swart, J., & Holliday, W. (2019). Cycling Biomechanics Optimization—the (R) Evolution of Bicycle
414 Fitting. *Curr Sports Med Rep*, 18(12), 490-496.
415 <https://doi.org/10.1249/JSR.0000000000000665>
- 416
- 417 Swart, J., & Holliday, W. (2019). Cycling Biomechanics Optimization—the (R) Evolution of Bicycle
418 Fitting. *Current Sports Medicine Reports*, 18(12). [https://journals.lww.com/acsm-](https://journals.lww.com/acsm-csmr/Fulltext/2019/12000/Cycling_Biomechanics_Optimization_the_R_.13.aspx)
419 [csmr/Fulltext/2019/12000/Cycling_Biomechanics_Optimization_the_R_.13.aspx](https://journals.lww.com/acsm-csmr/Fulltext/2019/12000/Cycling_Biomechanics_Optimization_the_R_.13.aspx)
- 420

- 421 Teed, Z., & Deng, J. (2020, 2020//). RAFT: Recurrent All-Pairs Field Transforms for Optical Flow.
422 Computer Vision – ECCV 2020, Cham.
- 423
- 424 Umberger, B. R., & Martin, P. E. (2001). Testing the planar assumption during ergometer cycling.
425 *Journal of Applied Biomechanics*, 17(1), 55-62.
426 <https://doi.org/http://journals.humankinetics.com/jab>
- 427
- 428 Xiao, B., Wu, H., & Wei, Y. (2018, 2018//). Simple Baselines for Human Pose Estimation and Tracking.
429 Computer Vision – ECCV 2018, Cham.
- 430
- 431
- 432

For Peer Review

433 **Tables**

434 **Table 1.** Mean \pm SD angles of the torso, hip, knee and ankle at the 3 o'clock and 6 o'clock crank
 435 positions determined using the Reference method, the MSRA method and the OpenPose method.

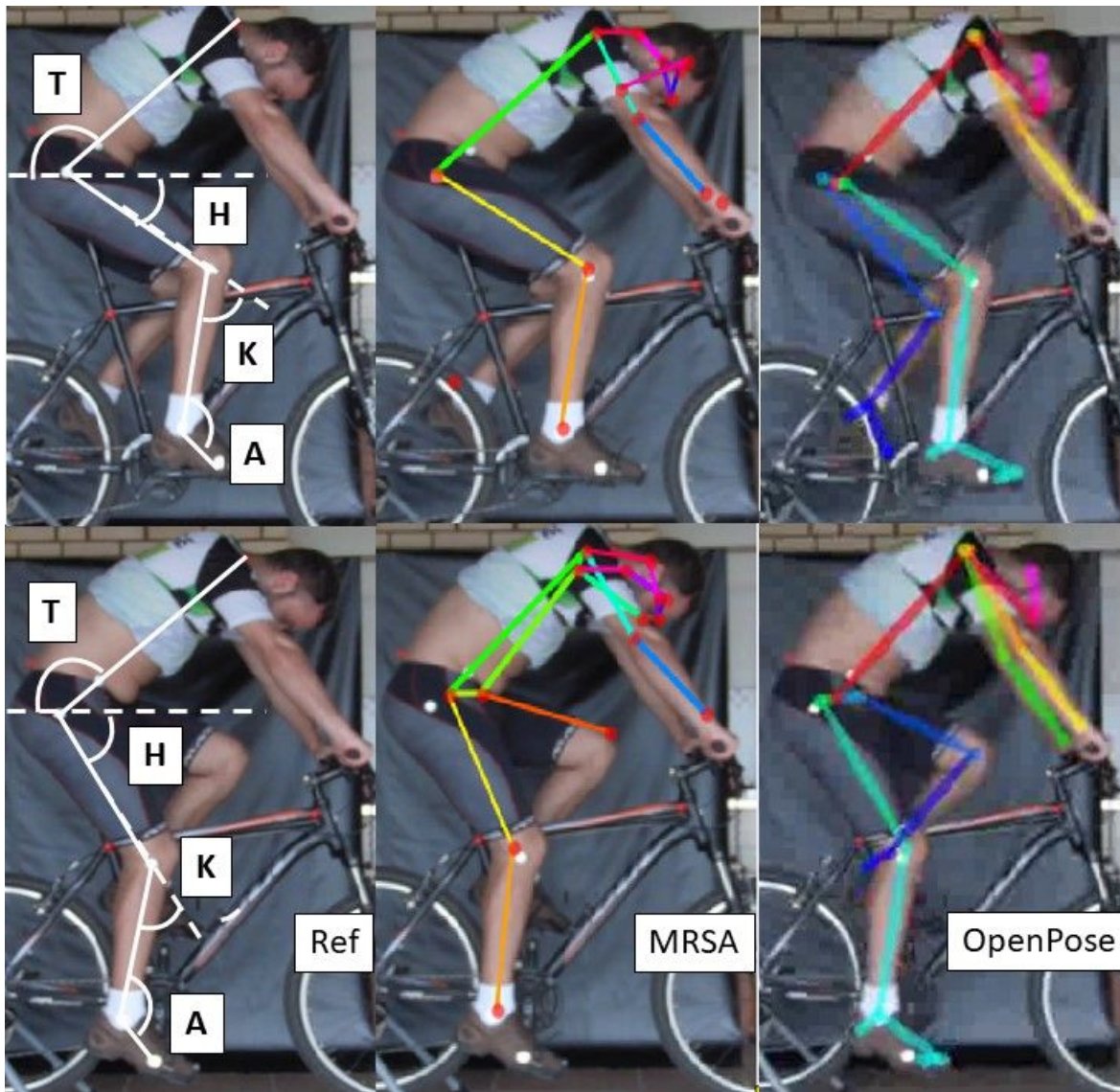
| 3 o'clock crank position | | | | |
|---------------------------------|--------------|-------------|--------------|--------------|
| Angles (°) | Torso | Hip | Knee | Ankle |
| Reference | 137 \pm 7 | 41 \pm 4 | 63 \pm 7 | 120 \pm 6 |
| MSRA | 139 \pm 7* | 32 \pm 5* | 75 \pm 9* | 113 \pm 9* |
| OpenPose | 135 \pm 9 | 40 \pm 3 | 64 \pm 5 | 122 \pm 3 |
| 6 o'clock crank position | | | | |
| Angles (°) | Torso | Hip | Knee | Ankle |
| Reference | 136 \pm 7 | 68 \pm 4 | 33 \pm 8 | 140 \pm 8 |
| MSRA | 141 \pm 7* | 65 \pm 5* | 37 \pm 11* | 137 \pm 11 |
| OpenPose | 134 \pm 9 | 68 \pm 4 | 35 \pm 7 | 141 \pm 8 |

436 * Indicates significant difference in relation to the Reference method.

437

438 Figures

439



440

441 **Figure 1.** Illustration of the measured angles and image from the skeleton created by the MSRA method.

442

443

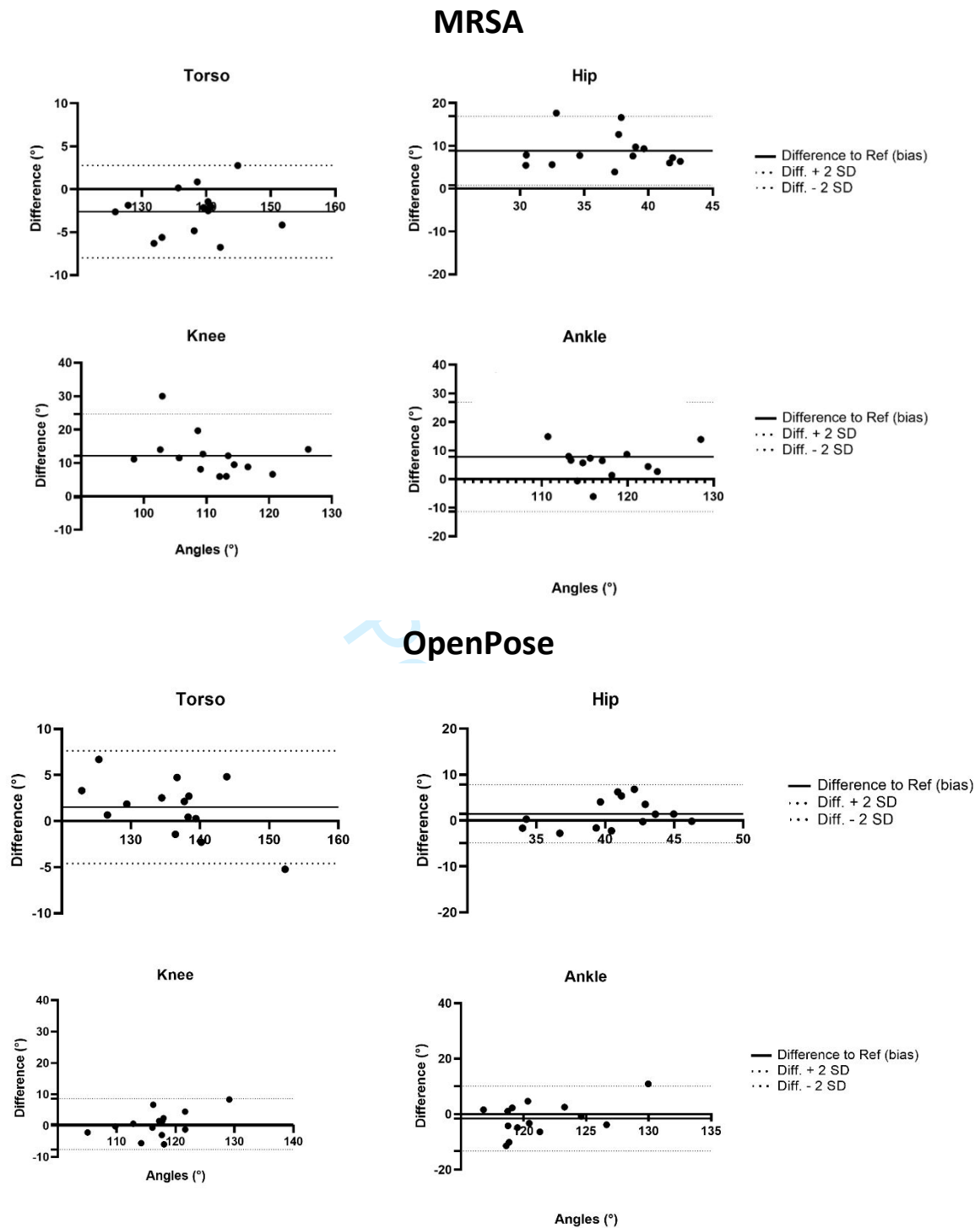
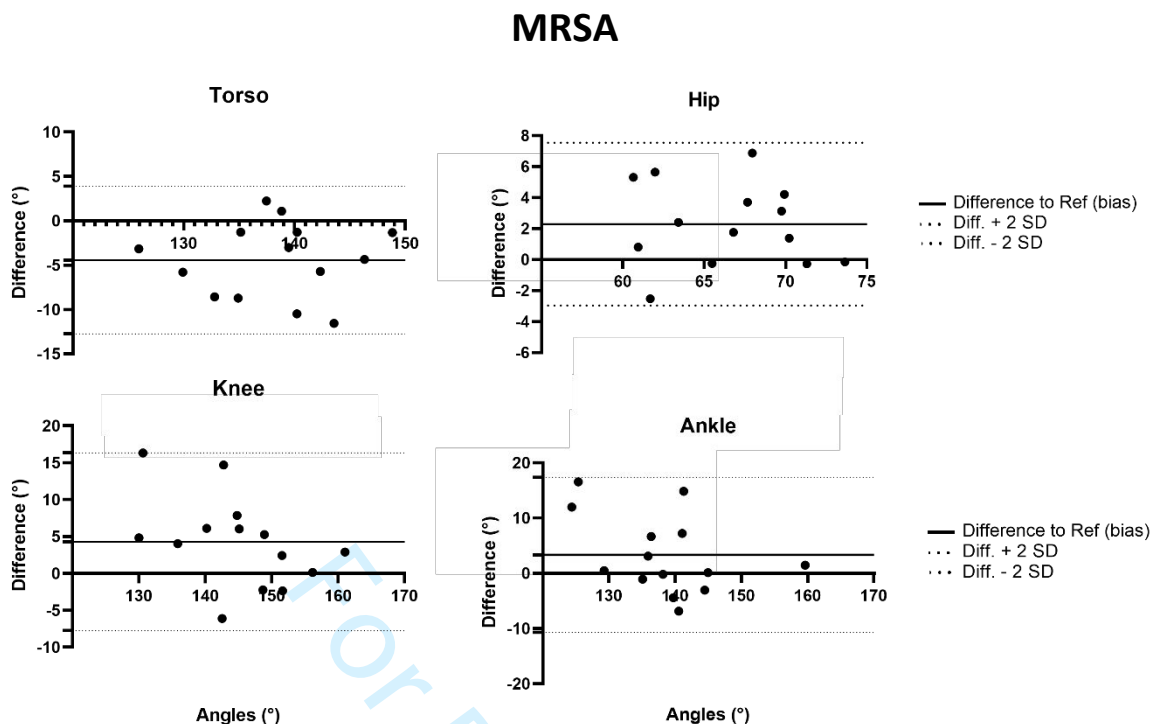


Figure 2. Bland-Altman plots comparing differences, mean bias (continuous lines) and limits of agreement (dotted lines) between the MRSa method and the Reference method (Ref – upper panel) and the OpenPose method and the Reference method (lower panel) for the 3 o'clock crank position.

444

445



OpenPose

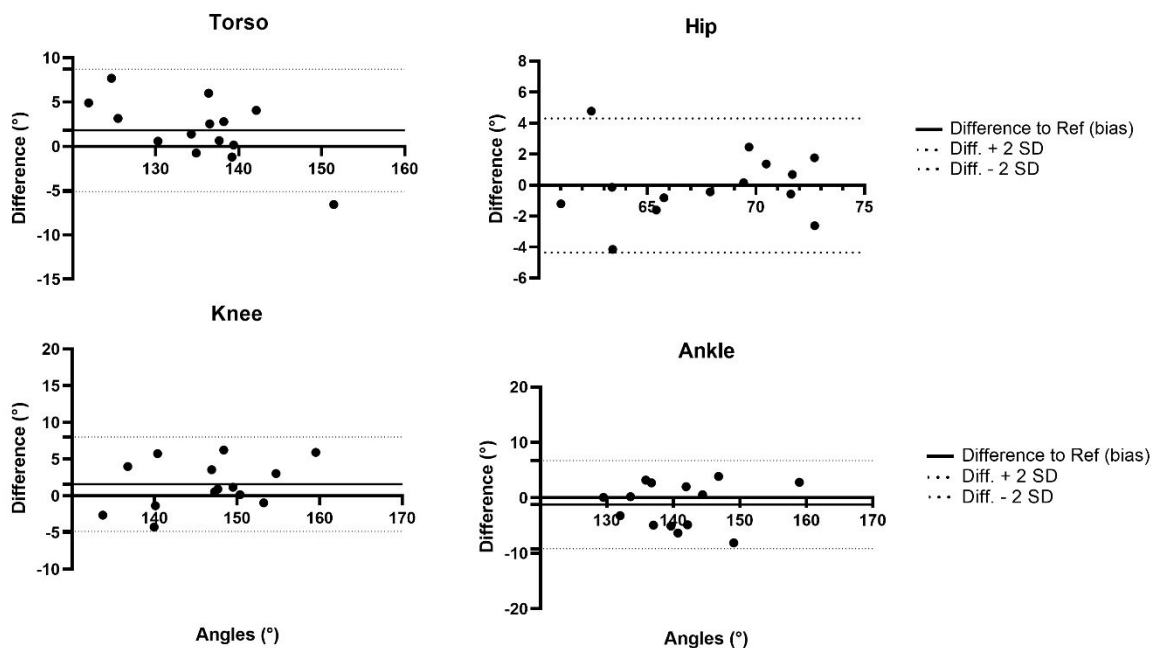


Figure 3. Bland-Altman plots comparing differences, mean bias (continuous lines) and limits of agreement (dotted lines) between the MRSA method and the Reference method (Ref – upper panel) and the OpenPose method and the Reference method (lower panel) for the 6 o’clock crank position.

446

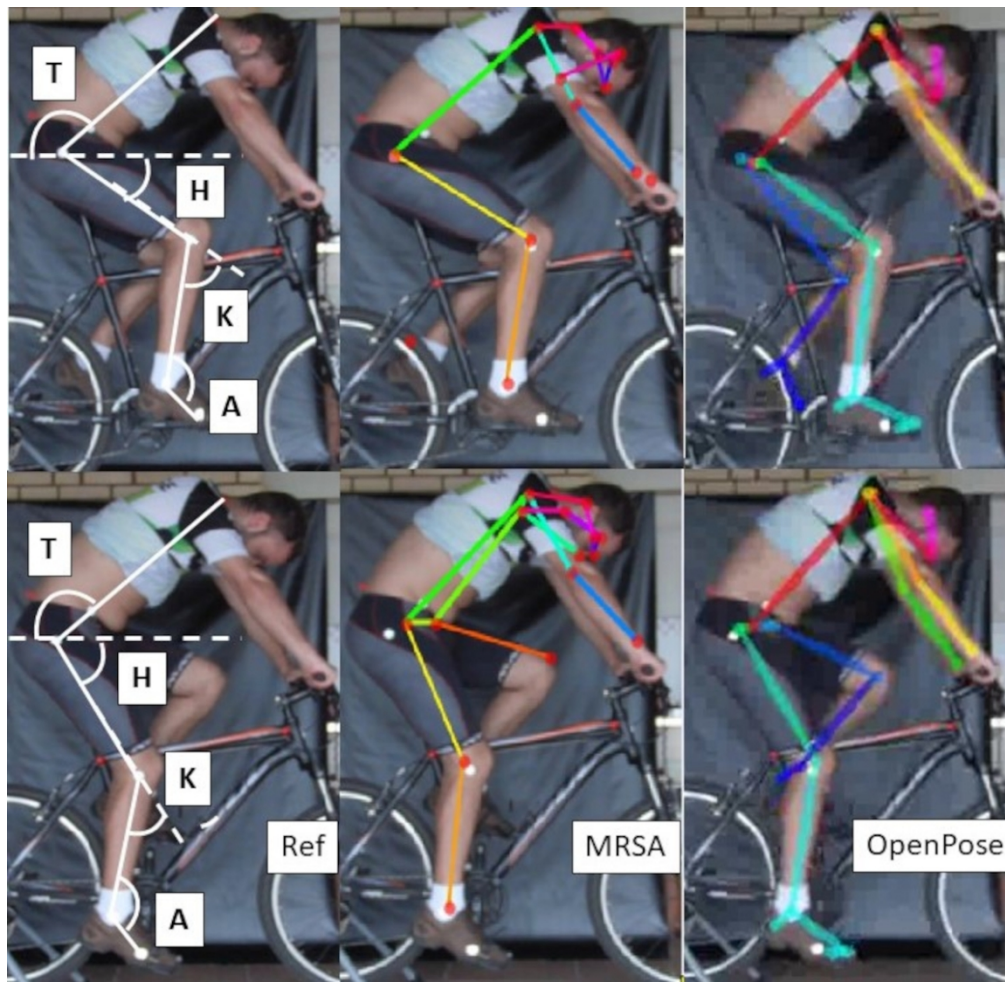


Figure 1

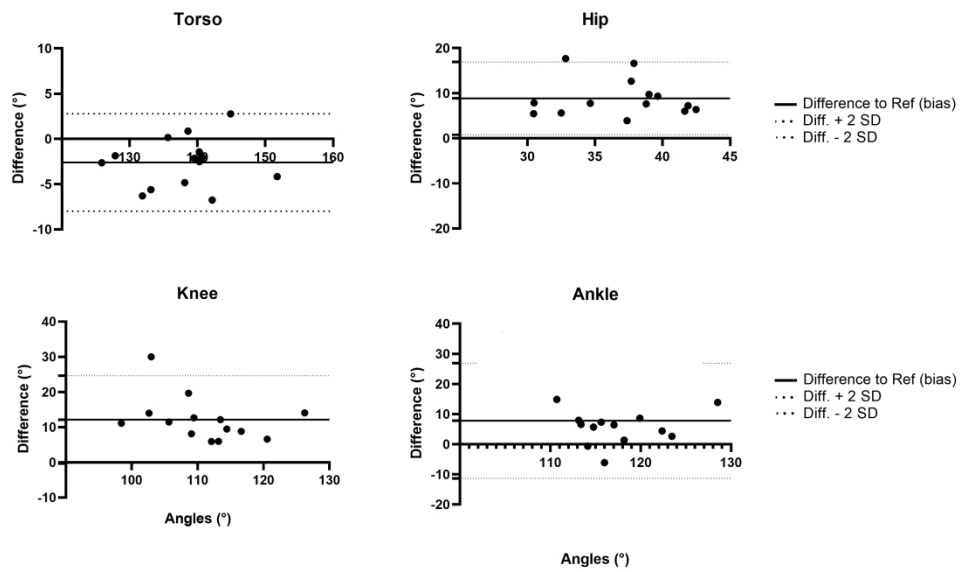


Figure 2- MRSA

284x173mm (300 x 300 DPI)

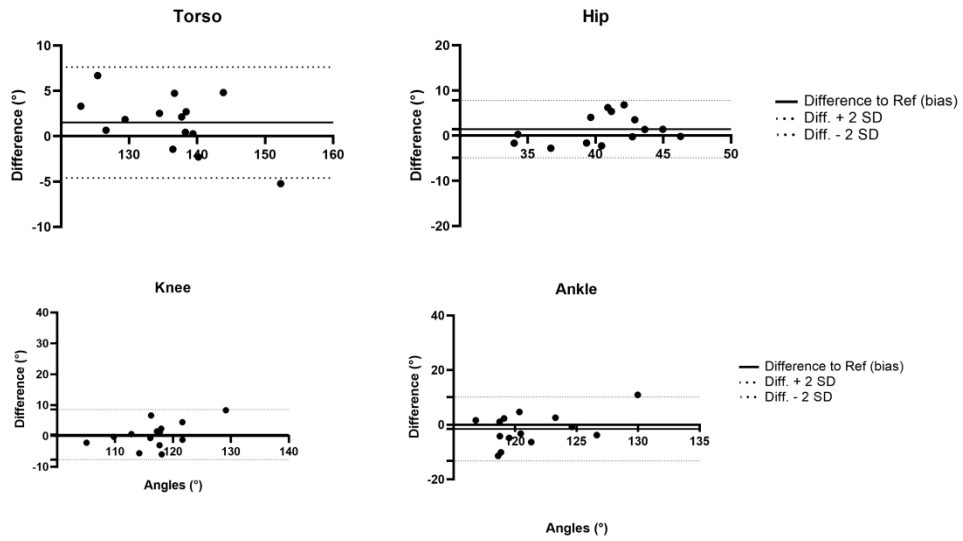


Figure 2 - OpenPose

284x164mm (300 x 300 DPI)

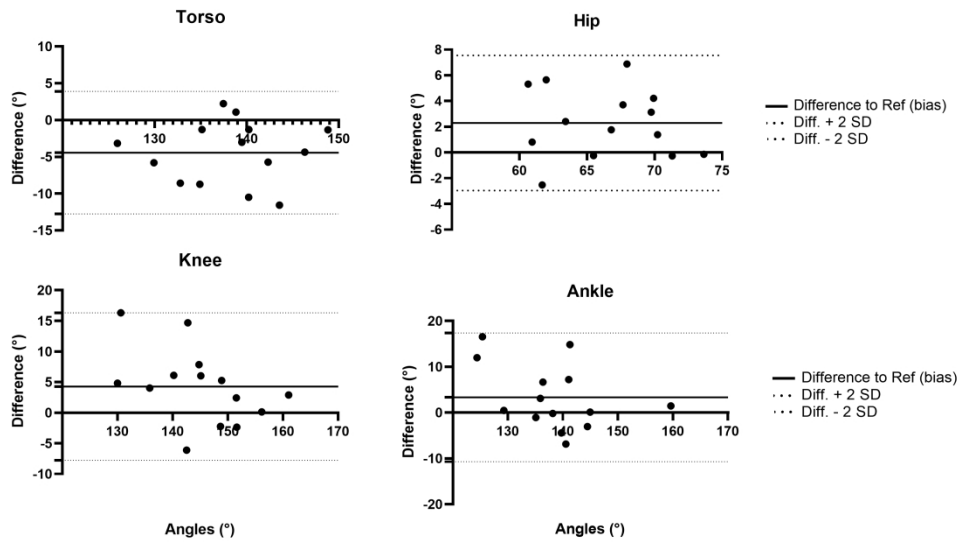


Figure 3 - MRSA

277x162mm (300 x 300 DPI)

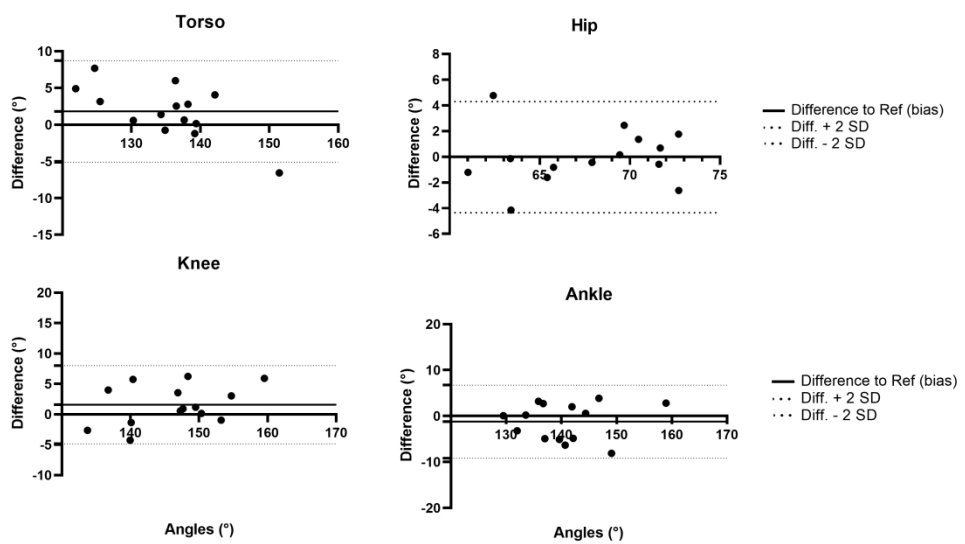


Figure 3 - OpenPose

279x162mm (300 x 300 DPI)